Proximodistal identity during vertebrate limb regeneration is regulated by Meis homeodomain proteins

Nadia Mercader[1,*], Elly M. Tanaka[2] and Miguel Torres[1,†]

[1]Departamento de Inmunología y Oncología, Centro Nacional de Biotecnología/CSIC, Campus de Cantoblanco, E-28049 Madrid, Spain
[2]Max Planck Institute for Molecular Cell Biology and Genetics, Pfotenhauer Strasse 108, 01307 Dresden, Germany
*Present address: EMBL, Meyerhofstrasse 1, D-69117 Heidelberg, Germany
†Author for correspondence (e-mail: mtorres@cnb.uam.es)

Accepted 11 July 2005

Development 132, 4131-4142
Published by The Company of Biologists 2005
doi:10.1242/dev.01976

Summary

The mechanisms by which cells obtain instructions to precisely re-create the missing parts of an organ remain an unresolved question in regenerative biology. Urodele limb regeneration is a powerful model in which to study these mechanisms. Following limb amputation, blastema cells interpret the proximal-most positional identity in the stump to reproduce missing parts faithfully. Classical experiments showed the ability of retinoic acid (RA) to proximalize blastema positional values. Meis homeobox genes are involved in RA-dependent specification of proximal cell identity during limb development. To understand the molecular basis for specifying proximal positional identities during regeneration, we isolated the axolotl Meis homeobox family. Axolotl Meis genes are RA-regulated during both regeneration and embryonic limb development. During limb regeneration, Meis overexpression relocates distal blastema cells to more proximal locations, whereas Meis knockdown inhibits RA proximalization of limb blastemas. Meis genes are thus crucial targets of RA proximalizing activity on blastema cells.

Key words: Axolotl, Retinoic acid, Vitamin A, Homeobox

Introduction

How cells interpret their position along the three axes of a morphogenetic field is fundamental to the correct patterning of developing and regenerating organs. This question has been studied extensively during vertebrate limb development (Tickle, 2003) and regeneration (Nye et al., 2003). Despite intensive effort in this field, how cells acquire positional information along the limb proximodistal (PD) axis remains poorly understood during both limb development (Duboule, 2002) and regeneration (Brockes, 1997).

Urodeles and anuran tadpoles are the only vertebrates able to regenerate amputated limbs completely. Following Spallanzani's description of this phenomenon in the 18th century (Spallanzani, 1768), scientists have tried to identify the mechanisms underlying limb regeneration and patterning of the growing blastema. As is the case during limb development, undifferentiated cells in the regenerating blastema acquire positional information de novo to reproduce the original pattern. In contrast to limb development, however, not every positional value needs to be recreated during regeneration, as the limb amputation can occur at any PD level and the blastema will reproducibly regenerate only the missing portion. A system of positional memory recorded in the mature limb is thought to instruct blastema cells of the exact PD level from which regeneration should take place (Stocum, 1984).

Classical experiments showed the role of RA as a major instructor of positional identity along the regenerating limb PD axis. When anuran tadpole or urodele limbs are amputated at the wrist and allowed to regenerate in an excess of RA, a whole PD axis develops rather than just the missing part, generating a tandem duplication (Maden, 1982; Niazi and Saxena, 1978). Duplications induced by decreasing amounts of RA result in increasing distalization of the proximal-most identity of the duplicated regenerate, showing the ability of RA to change positional values in a dose-dependent manner (Thoms and Stocum, 1984).

Cell affinity properties constitute a hallmark of PD positional identity of blastema cells (Nardi and Stocum, 1983). Consistent with its ability to proximalize regenerating limbs, RA reprograms blastema cell affinity properties towards a proximal identity (Crawford and Stocum, 1988) through the RARγ receptor isoform (Pecorino et al., 1996), downregulates the distal marker *Hoxa13* (Gardiner et al., 1995) and upregulates the proximal marker *Hoxd10* (Simon and Tabin, 1993). Recent results shed the first light on the molecular pathways controlling cell affinity that are activated by RA during limb regeneration. The GPI-anchored cell surface molecule Prod1 is more abundant in proximal than in distal blastemas, and is upregulated by RA (da Silva et al., 2002). Blocking Prod1 results in loss of the specific affinity properties of proximal blastemas, whereas overexpression of Prod1 in limb blastema cells causes them to translocate to more proximal positions, showing it contributes to the PD affinity code (Echeverri and Tanaka, 2005) Prod1 is also differentially expressed in the mature limb PD axis, suggesting that it forms part of the positional memory system (da Silva et al., 2002).

Some advances in the field of PD specification during limb development in amniotes came again from analyzing the RA pathway. During embryogenesis, RA is synthesized throughout the lateral plate mesoderm, but is excluded from the limb field as limb buds emerge from the trunk (Berggren et al., 1999; Niederreither et al., 1997). As determined by RA reporter transgene expression (Reynolds et al., 1991; Rossant et al., 1991), RA appears to be distributed in a proximal high-distal low gradient in the limb bud. RA is restricted proximally by limited diffusion from the trunk RA-producing region and by specific activation of the RA-degrading enzymes CYP26A1 and CYP26B1 in the distal limb (MacLean et al., 2001; Swindell et al., 1999). Study of *Raldh2*- and *CYP26B*-deficient mice revealed a role for RA in promoting limb outgrowth, as well as in limb PD patterning (Mic et al., 2004; Niederreither et al., 2002; Yashiro et al., 2004). Concurring with the view that RA instructs PD limb cell identities, distal limb bud region transplants generate proximal structures following RA treatment, and RA-exposed distal cells contribute to the formation of proximal skeletal elements (Ide et al., 1994; Mercader et al., 2000; Tamura et al., 1997). As during regeneration, cells of the developing limb bud display specific affinity according to their position in the PD axis (Ide et al., 1994), and RA can proximalize limb cell affinity in several experimental contexts (Ide et al., 1994; Mercader et al., 2000; Tamura et al., 1997).

Two closely related homeobox genes, *Meis1* and *Meis2*, are crucial targets activated by RA during PD limb axis patterning (Mercader et al., 2000; Yashiro et al., 2004). Early subdivision of the limb bud into proximal Meis-positive and distal Meis-negative domains is necessary for correct PD limb development; ectopic *Meis1* or *Meis2* overexpression abolishes distal limb structures (Capdevila et al., 1999), leads to a proximal shift of limb identities along the PD axis (Mercader et al., 1999), and proximalizes distal limb cell affinity properties (Mercader et al., 2000).

Meis genes encode transcription factors of the TALE class of homeodomain proteins. Members of this family share a three-amino-acid loop extension between homeodomain helices 1 and 2 (Bürglin, 1997). Meis proteins have an additional conserved N-terminal domain, through which they interact with members of a second TALE family, the PBC class, encompassing vertebrate proteins Pbx1 to Pbx4 (Chang et al., 1997; Knoepfler et al., 1997; Wagner et al., 2001). Meis-Pbx dimerization, as well as that of their insect counterparts, is required for nuclear localization of the proteins (Abu-Shaar et al., 1999; Berthelsen et al., 1999; Capdevila et al., 1999; Mercader et al., 2000; Rieckhof et al., 1997), and Meis-Pbx interaction is thus considered to be essential for their function.

During vertebrate limb regeneration, however, with the exception of Prod1, the elements in the molecular pathway activated by RA remain unknown. Here, we use recently developed electroporation methods (Echeverri and Tanaka, 2003; Echeverri and Tanaka, 2005; Schnapp and Tanaka, 2005) in the limb blastema to analyze the role of Meis genes in PD patterning during regeneration. We provide evidence of a role for Meis genes as crucial targets of RA proximalizing activity during limb regeneration. Our results show that the RA-Meis pathway, active during limb development, is essential to specify RA-induced proximal fates during limb regeneration.

Materials and methods

Animal handling, RA administration and tissue collection

We established an axolotl colony (*Ambystoma mexicanum*) from 40 founder animals imported from Indiana University (USA). For electroporation, blastemas were generated on animals with a snout-to-tail length of 3-5 cm. For RA treatment and RNA or protein extraction, 4-7 cm-long animals were used. Experimental animals were anesthetized in 0.01% ethyl-p-amino benzoate (Sigma) prior to amputation and limbs were allowed to regenerate at room temperature. For RA treatment, all-trans RA (Sigma) dissolved in DMSO was injected intraperitoneally (100 μg/g body weight) on day 4 post-amputation (Thoms and Stocum, 1984). To study the effect of RA during limb development, tadpoles were immersed (10-24 hours) in 10 mM all-trans RA in swimming water.

Cloning axolotl *Meis* and *Pbx* genes

Primers used for axolotl *Meis1* and *Meis2* amplification from proximal medium bud blastema cDNA (*Meis1*) and whole tadpole cDNA (*Meis2*) were: Meis1, 5′-ACTAGTGATTCTGCACTC, and 5′-CATGTAGTGCCATTGCCCCTC; Meis2, 5′-CTTCAACGAG-GACATCGCGGTC and 5′-TTGGGGAATATGCCTCTTTTCTTC. Full-length *Meis* sequences were completed by 5′ and 3′RACE using the following primers.

For 5′RACE: Meis1, 5′-TGCGATTGGTTAACTAGATGGT and 5′-GATTGGTTAACTAGATGGTGTTAC; Meis2, 5′-AGCGTAG-GAACAGGGCGAAGTC and 5′-GCATCACGACAGGCCGCAC-ATC.

For 3′RACE: Meis1, 5′-GTAAGTCAAGGTACACCA and 5′-CCATGGGAGGATTTGTGA; Meis2, 5′-GTGAACCAAGGGGAC-GGGC and 5′-ACAGCGTGGCCTCTCCTG.

The axolotl Pbx1 full-length sequence was identified in the axolotl EST sequencing project database (Habermann et al., 2004). Axolotl *Meis1*, *Meis2* and *Pbx1* nucleotide sequences have been submitted to GenBank with accession numbers DQ100364, DQ100365 and DQ100366.

In situ hybridization

The following probes were used: *axoMeis2* (+337 to +828) and *axoHoxa13* (+552 to +834). Whole-mount in situ hybridization was performed as described (Wilkinson and Nieto, 1993), with proteinase K treatment (10 μg/ml) for 10 minutes for the youngest embryos and 15 minutes for stage (St) 36 to St43 tadpoles.

For in situ hybridization on sections, 12 μm cryosections were collected on Superfrost slides, air-dried (2 hours), and hybridized as described (Myat et al., 1996).

Immunohistochemistry and antibodies

Tissue samples were collected and fixed immediately in 4% paraformaldehyde (PFA; overnight, 4°C), rinsed in PBS and dehydrated in methanol. Specimens were rehydrated to PBS, immersed in 30% sucrose in PBS (overnight, 4°C), OCT-embedded, sectioned (12 μm) on a cryostat and collected on Superfrost slides. Prior to immunohistochemistry, slides were air-dried (30-60 minutes, RT), refixed in ice-cold acetone (2 minutes, 4°C), rinsed in PBS, treated with 100 mM glycine in PBS (30 minutes) and washed in PBT (PBS 0.1% Tween-20). Sections were permeabilized with 0.05% Triton X-100 in PBS (10 minutes), followed by a PBT wash (5 minutes). A second permeabilization step was performed with PBS:DMSO (1:1; 8 min), and a PBT wash. Slides were blocked in 10% goat serum (overnight at 4°C), incubated sequentially with the primary antibody, with biotin-conjugated secondary antibody and with streptavidin-Cy3 (Jackson) (1 hour each, room temperature).

Anti-Meis-a antibody was generated in rabbits with a synthetic peptide corresponding to the conserved C-terminal domain of Meis1a and Meis2a/Meis2b isoforms (GMNMGMDGQWHYM). Anti-Meis1 and -Meis2 antibodies were raised in rabbits using the peptide

sequences HAARSMQPVHHLNHGPP and HAPRPIPPVHHLNHGPP, respectively. Anti-Pbx1/Pbx2/Pbx3/Pbx4 was purchased from Santa Cruz Biotechnology and used at 20 μg/ml. Overexpressed tagged Meis1, Meis2 and Pbx1 proteins were detected using anti-FLAG (Sigma) and anti-Myc monoclonal antibodies.

Quantitative RT-PCR and western blot analysis

For western blot, blastemas were lysed in RIPA and 15 μg protein lysate was transferred to nylon membranes and counterstained with Ponceau Red to visualize total protein.

Quantitative PCR was performed on an ABIPrism 7700 thermocycler (Applied Biosystems) applying 1 cycle at 50°C for 2 minutes, 1 cycle at 95°C, 10 minutes, 40 cycles at 95°C, 15 seconds, and at 67°C, 90 seconds, followed by 1 cycle at 95°C, 15 seconds, and at 60°C, 15 seconds, and a final step at 95°C, 15 seconds. For each cDNA sample, two dilutions (1/50 and 1/500) were amplified in duplicate. The following primers were used:

Meis1, 5′-CCATCTACGGACACCCCCT and 5′-GGAAGAACACACGTCCCCG;

Meis2: 5′-AGTGGAGGGCACGCTTCT and 5′-GCTTCTTGTCTTTGTCCGGGT;

Hoxa13: 5′-TCTGGAAGTCCTCTCTGCCG and 5′-TCAGCTGGACCTTGGTGTACG;

Ef1α: 5′-CGGGCACAGGGATTTCATC and 5′-TGCCGGCTTCAAACTCTCC. Amplification reactions were carried out simultaneously using SYBR Green PCR Master Mix (Applied Biosystems). c_t values obtained for experimental primer sets were normalized with c_t values for EF1α control primers (Livak and Schmittgen, 2001).

Electroporation of DNA constructs and antisense morpholino into limb blastemas

Axolotl *Meis1* and *Meis2* cDNA cloned into pCMVTag2b and axolotl *Pbx1* cloned into pCMVTag3b vectors (Stratagene) were diluted in PBS (0.25 μg/μl), together with a CMV-nuclear EGFP reporter plasmid (0.05 μg/μl). Using a microinjector (Inject+Matic, Geneva), DNA solution (~7 nl), with Fast Green added to improve monitoring, was injected at three different blastema sites to ensure homogeneous distribution. Immediately after injection, five pulses were given (5 mseconds, 150 V/cm each) using flat circular electrodes (3 mm diameter) with an electroporator (BTX ECM-830, San Diego). To count GFP-positive cells, limbs were fixed in 4% PFA (overnight, 4°C), soaked in 30% sucrose in PBS (2 hours) and OCT-embedded. Longitudinal cryosections (30 μm) were collected on slides, air-dried (2-6 hours), fixed in ice-cold acetone (2 minutes), rinsed in PBS and mounted in anti-fading mounting medium.

Fluorescein-coupled antisense morpholino oligonucleotides (MOs) were designed against 5′-coding regions of *axoMeis1* (5′-AAGTCGTCGTACCTTTGCGCCATCG) and *axoMeis2* (5′-GGAGTTCATCGTACAGAAACATGAT) (Gene Tools, Corvallis, OR). A fluorescein-coupled standard MO was used as control. MO were diluted in water and stored at –20°C as a 5 mM stock solution. For injection, MO were diluted to 1.5 mM in PBS and heated (68°C) for 10 minutes prior to use. Injection and electroporation were as indicated above for DNA constructs.

Results

Meis and Pbx distribution and regulation during axolotl limb development

Using primers against conserved sequences of mouse Meis cDNA at low stringency, we amplified axolotl cDNA fragments corresponding to the three vertebrate Meis genes. We subsequently obtained full cDNA sequences of axolotl *Meis1* and *Meis2*, and a partial *Meis3* sequence, by 5′ and 3′ RACE. Axolotl Meis2, Meis1 and Meis3 proteins show 99%, 97% and 90% identity to their respective mouse counterparts. Whole-mount mRNA in situ hybridization showed a *Meis2* expression pattern in axolotl embryonic central nervous system (CNS) that is similar to that described in mouse embryos (Fig. 1A-D). Two major Meis isoforms differing in the C-terminal region are generated by alternative splicing in vertebrates, a short C terminus form (corresponding to mouse Meis1a, Meis2a and Meis2b) and a long C terminus form (corresponding to mouse Meis1b, Meis2c and Meis2d). Although our strategy was designed to clone either isoform, from several cDNA sources, we amplified mainly the short isoform-encoding cDNA of *Meis1* and *Meis2*, suggesting that this is the predominant form in axolotls.

An antibody that recognizes an epitope conserved in all short isoforms of mouse and axolotl Meis proteins (anti-Meis-a) specifically detects a nuclear signal in the embryonic CNS, in a pattern that correlates with *Meis2* mRNA distribution (Fig. 1E-H). Using this antibody, we examined Meis protein distribution during limb outgrowth. At stage H36, when the limb bud has just formed, the Meis protein signal is strong, nuclear and uniformly distributed throughout the limb bud (Fig. 1I). From stage 40, we found that the limb bud was subdivided into two regions defined by Meis protein distribution, a proximal region retaining a strong nuclear Meis-a signal and a distal region showing a low, diffuse Meis-a signal with cytoplasmic enhancement (Fig. 1J). During subsequent limb bud stages, we found progressive growth of the distal, non-nuclear Meis region and maintenance of the proximal confinement of nuclear Meis expression (Fig. 1K). In early limb buds, Meis-a signal was detected in a nuclear pattern in the ectoderm (Fig. 1I). Ectodermal expression has been described in the mouse for *Meis2* (Oulad-Abdelghani et al., 1997) and *Meis1* (N.M. and M.T., unpublished). *Meis2* mRNA distribution during limb development was uniform with no proximal restriction at any stage in the mesenchyme, and was weak or absent in the ectoderm (Fig. 1N-P). These observations suggest that Meis protein expression could be subject to post-transcriptional, and/or subcellular distribution, control during limb development. We observed no expression by in situ hybridization using different *Meis1* probes in the embryo, whereas *Meis3* was detected in the CNS, but was not detected in developing limbs (not shown). We cannot disregard, however, the fact that technical problems might underlie our inability to detect *Meis1* transcripts in situ, as RT-PCR analysis indicated the presence of *Meis1* mRNA in embryos (data not shown). *Meis1* expression may therefore also contribute to the proximal enrichment in Meis-a signal, as well as to the ectodermal Meis expression. We also analysed the expression of Pbx proteins during limb development using an antibody that recognizes a conserved epitope present in all Pbx proteins (Pbx1-4). Nuclear Pbx expression was detected ubiquitously along the limb bud PD axis, with higher expression in the proximal versus distal regions of the bud (Fig. 1M).

We next tested whether Meis expression was RA-regulated during axolotl limb development. Exposure of stage 43 axolotl larvae to 0.12 mM RA in the swimming water for 22 hours produced an extension of the Meis protein expression domain and an enhancement of its nuclear signal (Fig. 1L), as well as an overall increase in *Meis2* mRNA expression (Fig. 1Q).

These results indicate that the proximal restriction of Meis activity during limb development and its positive regulation by

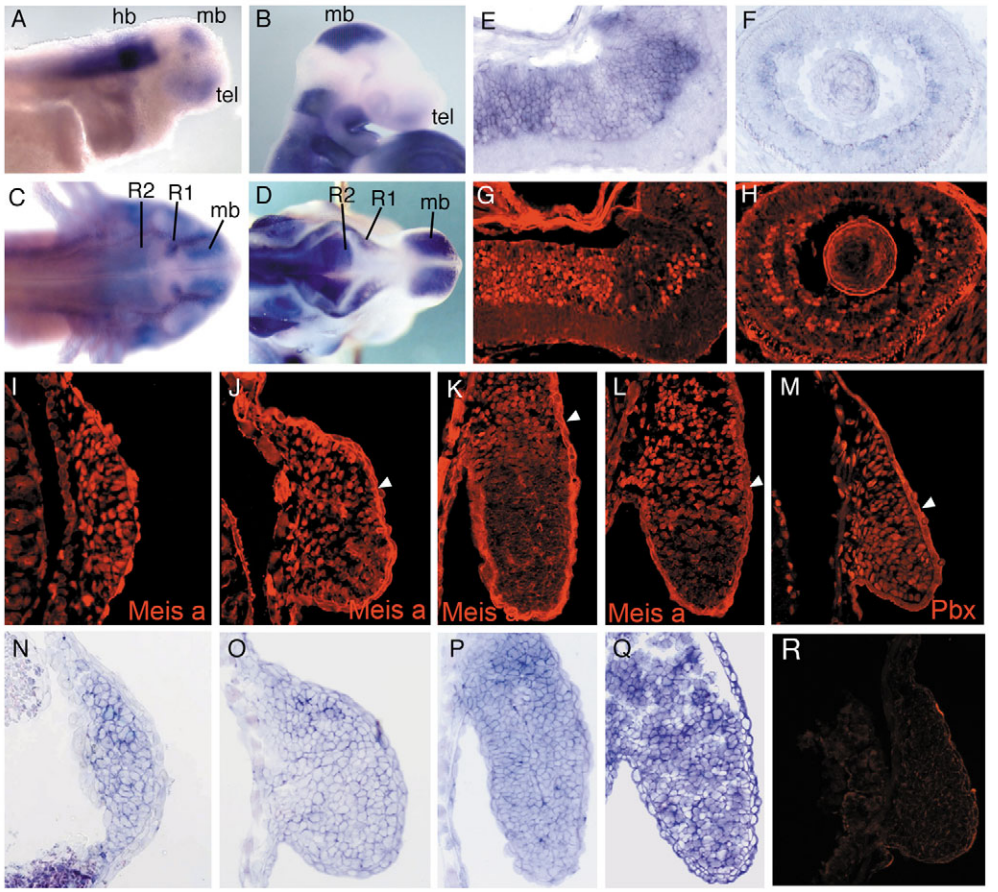

Fig. 1. Meis expression and regulation is conserved during axolotl embryogenesis. (A-D) Whole-mount in situ hybridization of late tail bud (A, lateral view) and prehatching (C, dorsal view) axolotl embryos, compared with E9.5 (B) and E10.5 (D) murine embryos, showing *Meis2* expression in the head. (E-H) *Meis2* in situ hybridization (E,F) and immunohistochemistry using Meis-a antibody (G,H) on adjacent stage (St) 41 sagittal hindbrain (E,G) and eye sections (F,H). (I-L,N-Q) Analysis of Meis expression during axolotl limb development. Meis-a immunohistochemistry (I-L) and in situ hybridization with a *Meis2* riboprobe (N-Q) on adjacent cryosections from St36 (I,N), St40 (J,O) and St43 (K,L,P,Q) limb buds. (L,Q) Limb bud sections from a St43 axolotl larva treated with 0.12 mM retinoic acid (RA) for 22 hours. Arrowheads indicate the distal limit of nuclear Meis expression in the limb bud. (M) Anti-Pbx1/2/3/4 immunohistochemistry on a St42 limb section. Arrowhead indicates the limit between proximal high and distal low nuclear Pbx expression. (R) Negative control for immunohistochemical stainings. hb, hindbrain; mb, midbrain; R1, rhombomere 1; R2, rhombomere 2; tel, telencephalon.

the RA pathway are conserved between the axolotl and amniotes.

Meis expression and regulation by RA during limb regeneration

To analyze Meis pathway involvement in PD patterning during regeneration, we studied the Meis gene expression pattern in limb blastemas amputated at different PD positions. In situ hybridization showed no differences in *Meis1* and *Meis2* mRNA expression levels between proximal and distal blastemas (data not shown). Nonetheless, real-time PCR (RT-PCR) showed that *Meis1* and *Meis2* transcripts are more abundant in proximal than in distal medium bud blastemas, by a factor of 3.4 and 2.5, respectively (Fig. 2A). In these experiments, *Hoxa13* was more abundant in distal than in proximal blastemas (Fig. 2A), as described previously (Gardiner et al., 1995). *Meis3* was not detected by RT-PCR in blastemas from any axial amputation level or stage (not shown). RA treatment of distal blastemas increased *Meis1* and *Meis2* transcripts by 2.3- and 2.2-fold, respectively (Fig. 2A). As reported elsewhere (Gardiner et al., 1995), *Hoxa13* expression was repressed after RA treatment of distal blastemas (Fig. 2A).

Similar samples were analyzed by western blot to determine protein variations. Meis proteins detected using anti-Meis-a were 4-fold more abundant, and Meis2 was 3-fold more abundant, in proximal versus distal blastemas (Fig. 2B). RA treatment of distal blastemas elevated Meis protein levels over those in proximal blastemas; Meis proteins detected with anti-Meis-a increased 6-fold, whereas Meis2 increased 4.5-fold compared with proximal blastemas (Fig. 2B). In immunohistochemical analysis, an endogenous Meis-a signal was not detected in distal blastemas from untreated animals at any regeneration stage (Fig. 2C,F and not shown); however, a nuclear Meis-a signal was detected in the majority of distal blastema cells three days after RA treatment (Fig. 2D,G). The Meis-a nuclear signal was stronger and more widespread in the blastema 6 days after RA treatment. At this stage, however, a narrow distal Meis-a low-expression area was observed (Fig. 2E,H). The strong Meis-a signal persisted 9 days post-injection

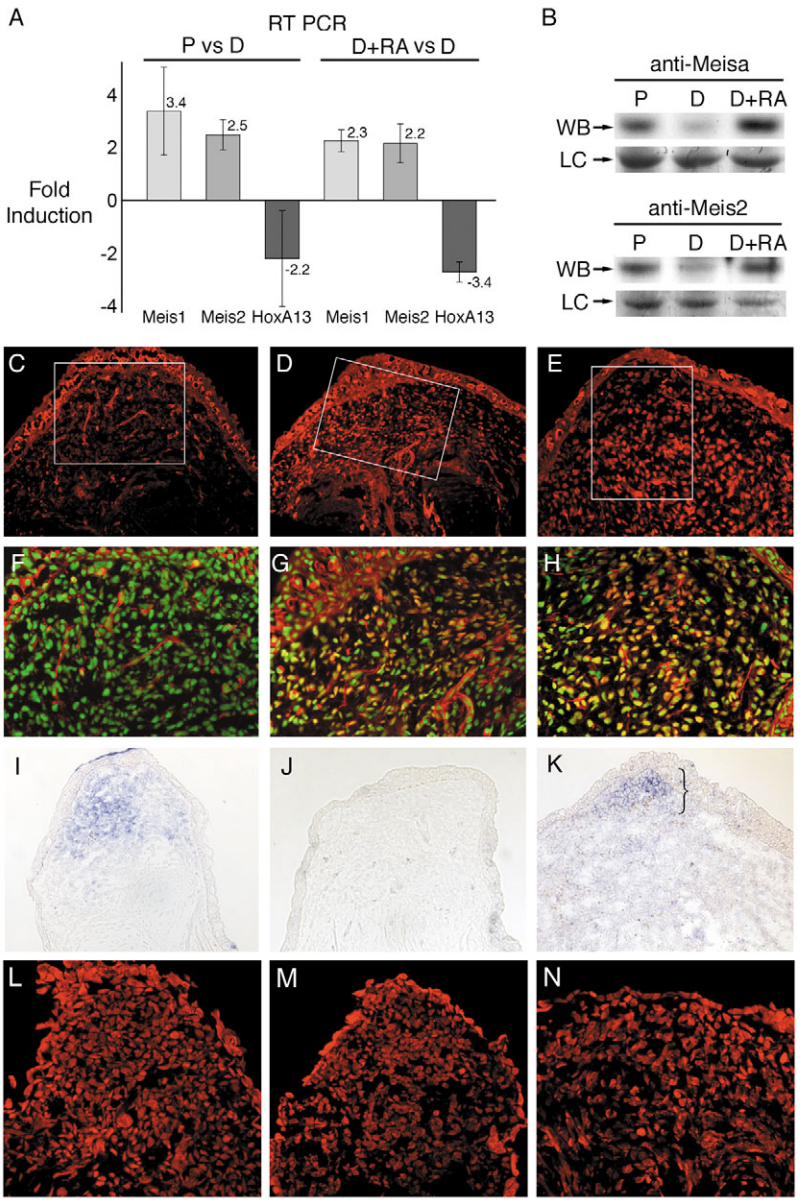

Fig. 2. Meis expression and regulation by RA during limb regeneration. (A) Comparative results of quantitative RT-PCR amplification of *Meis1*, *Meis2* and *Hoxa13* from proximal (P), distal (D) and RA-treated distal (D+RA) medium bud blastema cDNA. (B) Western blot analysis of proximal (P), distal (D) and RA-treated distal (D+RA) blastemas. LC, loading control. RA treatment in A and B was maintained for 3 days before analysis. (C-H) Immunohistochemical detection of Meis-a (red) and nuclei (green) are shown on cryosections of distal blastemas at 4 days post-amputation (C,F), or distal blastemas 3 (D,G) and 6 (E,H) days after RA injection. (F-H) Higher magnification of boxed regions in C-E. (I-K) *Hoxa13* in situ hybridization of blastemas treated as in C-E. Bracket in K indicates the distal blastema domain in which *Hoxa13* expression is reactivated. (L-N) Anti-Pbx1/2/3/4 immunohistochemistry on proximal (L), distal (M) and RA-treated distal (N) medium bud blastemas, revealing nuclear Pbx localization throughout the blastema.

in proximal blastema regions (not shown). The *Hoxa13* expression pattern was complementary, with broad expression in blastemas from untreated animals, disappearing 3 days after RA treatment and re-appearing at 6 days post-treatment in the Meis-a low-expression area (Fig. 2I-K).

These results showed that Meis expression is regulated in limb blastemas depending on the PD amputation position, and that RA activates Meis mRNA and protein expression levels during regeneration. By contrast, in early to medium bud stage blastemas, a homogeneous nuclear Pbx expression pattern was observed, which did not increase significantly after proximalization of distal blastemas with RA (Fig. 2L-N and data not shown).

Analysis of Meis mRNA or protein levels in tissues from several PD positions of the mature limb showed no differences for Meis1 or Meis2 (not shown). We thus found no direct evidence that Meis activity takes part in positional memory, although we cannot exclude that regulation of Meis activity in the mature limb takes place at the subcellular localization level.

Meis proteins proximalize the affinity properties of limb blastema cells

We used overexpression experiments for functional testing of Meis protein involvement in PD patterning during limb regeneration. Because Meis function may require the presence of a Pbx partner, we included co-expression of Meis together with Pbx1 in our analysis. For these experiments, we used a full-length Pbx1 cDNA identified in the axolotl cDNA sequencing project (Habermann et al., 2004). Expression plasmids driving different Meis or Pbx1 proteins fused to the FLAG epitope or driving EGFP (Fig. 3A) were electroporated into the limb blastema 6 days after amputation. When overexpressed without Pbx1, Meis proteins were detected only until 48 hours after electroporation. By contrast, when introduced together, both Pbx1 and Meis proteins were detected until 5 days after electroporation (Fig. 3B). Meis or Pbx1 proteins were no longer detected from day 6, but EGFP persisted up to 20 days post-electroporation (Fig. 3C and not shown). The proportion of electroporated cells ranged from 5 to 10% of blastema cells, precluding the use of this approach to study the consequences of Meis/Pbx1 overexpression in pattern formation (Fig. 3B,C). By contrast, the persistence of EGFP detection allowed us to determine the contribution of electroporated cell descendants to the regenerated limbs. Proximal blastemas were electroporated with different combinations of Meis/Pbx1 and EGFP expression vectors, and their contribution was compared with that of GFP-only-electroporated control cells. Control cells were widely dispersed throughout the PD extension of the regenerate (Fig. 3D-F). By contrast, any combination containing Meis1a or Meis2a promoted aggregation of electroporated cells and their preferential location in proximal regenerate regions, both evident from 3 days after electroporation (Fig. 3G-I and data not shown).

To quantify the results, regenerated limbs were sectioned horizontally and positive cells scored in the different PD regions. Any combination containing Meis1a or Meis2a produced a higher frequency of GFP-positive cells in proximal regions compared with controls (Fig. 3J). Whereas positive cell frequency in distal stylopod plus proximal zeugopod was 25% in controls, it was between 53 and 70% in Meis1a- or Meis2a-electroporated blastemas (Fig. 3J). Meis1b isoform activity in this assay was tested by electroporating the murine protein. In contrast to the results for Meis-a, we observed no effect of Meis1b on PD cell distribution (Fig. 3J). Pbx1 alone neither altered the relative PD distribution of electroporated cells nor contributed appreciably to the Meis effect on PD cell distribution (Fig. 3J). This result is consistent with its expression during limb regeneration, where no differential Pbx expression could be detected between proximal and distal blastemas. On the contrary, a homogeneous nuclear Pbx expression pattern in early to medium bud stage blastemas was observed, which did not increase significantly after proximalization of distal blastemas with RA (Fig. 2L-N and data not shown).

In some experimental conditions studied, positive cell counts in total limb were markedly reduced when compared with controls (Fig. 3K). This phenomenon was most evident in Meis-only electroporated limbs, such that absolute cell numbers in proximal regions increased only marginally compared with controls (Fig. 3K). Co-electroporation with Pbx1 rescued total numbers of GFP-positive cells, resulting in

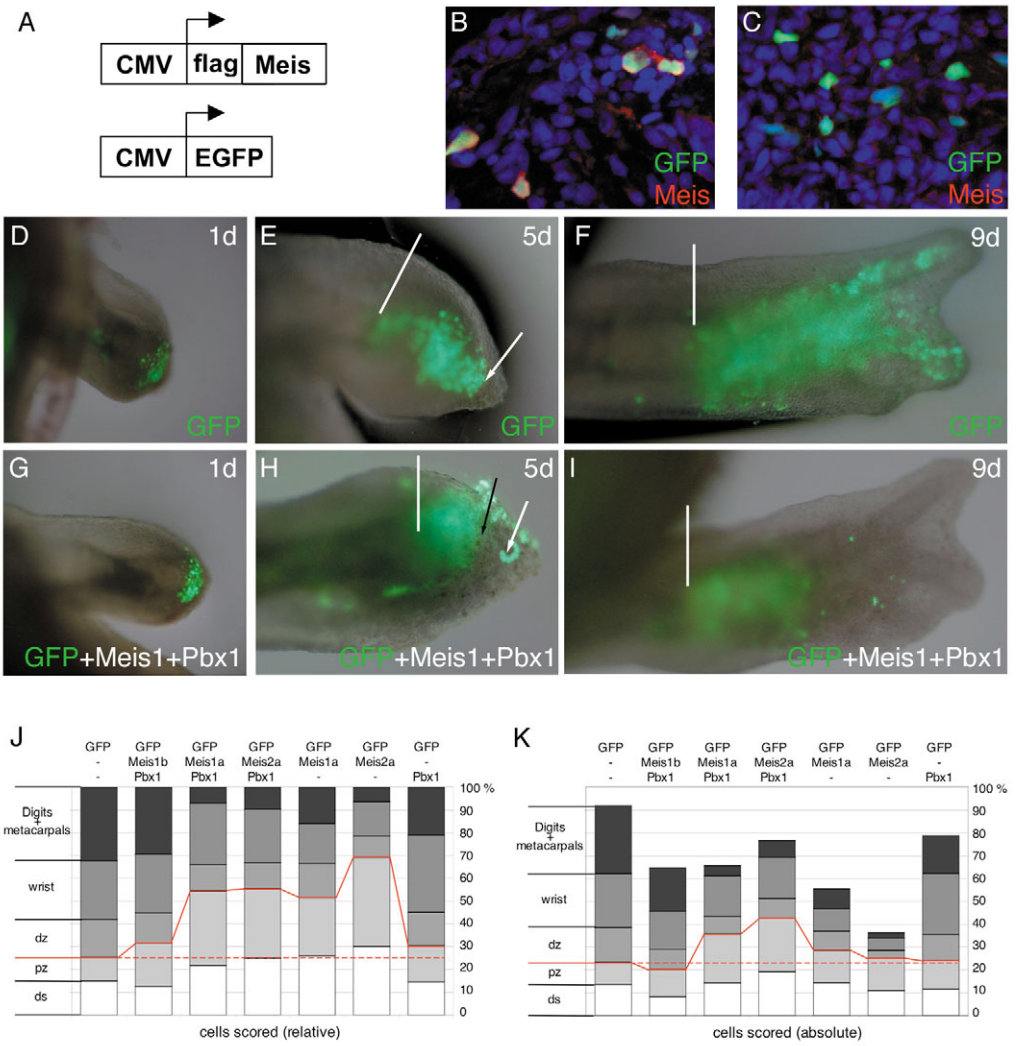

Fig. 3. In vivo fate mapping of Meis-overexpressing cells in limb regenerates. (A) Constructs used for electroporation. (B,C) Immunohistochemistry on blastema sections 1 (B) and 6 (C) days after electroporation; Meis (red), GFP (green), nuclei (blue). (D-I) Time-lapse analysis of electroporated cells during proximal limb regeneration. Early bud mid-humerus blastemas electroporated with GFP (D-F) or Meis1+Pbx1+GFP plasmids (G-I) at different times post-electroporation. White lines indicate the amputation plane; white arrows, the limit between mesenchyme and the ectodermal cap; black arrow in H, the distal-most position of electroporated cells. (J,K) Diagram of the relative contribution of electroporated cells to the PD segments (indicated at left). (J) Proportions relative to the total number of cells scored in each condition; (K) proportions relative to the total number of cells observed in control limbs. The construct combinations used are indicated above. The solid red line indicates the percentage of electroporated cells contributing to regions proximal to mid-zeugopod in controls; the dotted red line indicates this percentage in different experimental conditions. dz, distal zeugopod; pz, proximal zeugopod; ds, distal stylopod.

a net increase in absolute cell number in proximal regions (Fig. 3K).

The proximal-preferential distribution of Meis-expressing cells may result from a number of possible cellular effects induced by Meis overexpression, including distal-specific underproliferation, increased death of Meis-electroporated cells, relocation of Meis-expressing cells to proximal limb regions, or combinations of these. Proliferation and cell death rates of electroporated limbs were analyzed at different regeneration stages, with no notable differences between control and experimental conditions, or between proximal and distal blastema regions (data not shown). Undetectable differences in proliferation or cell death rates could nonetheless cause a significant difference in cell number if they accumulated during the 9-day experimental period.

To determine directly whether proximal relocation was a principal cause of the cell redistribution, we set up focal electroporation to target specific regenerate subregions (Fig. 4A,B). Focal electroporation of control plasmid in the distal third of the medium bud limb blastema (closer than 350 μm to the apical ectodermal cap) resulted in GFP-positive cells that contributed almost exclusively to distal regions, with very few regenerates showing GFP-positive cells in zeugopod (2/12) or stylopod (1/12) (Fig. 4I). By contrast, similar electroporation with Meis2a, alone or with Pbx1, resulted in a large proportion of limbs containing GFP-positive cells in zeugopod (20/23) or stylopod (14/23) (Fig. 4E,F,I). Total cell counts in each PD segment in horizontal sections of regenerates showed that Meis2a, alone or with Pbx1, produced proximal relocation of approximately 40% of the electroporated cells (Fig. 4J).

Similar experiments using mass electroporation in blastemas from wrist-level amputations showed that Meis1a/Meis2a, alone or with Pbx1, induced cell aggregation and confinement to the proximal-most region of the regenerate (Fig. 4C,D,G,H and data not shown). Control focal electroporation in distal regions of late bud proximal amputation blastemas produced cells contributing mainly to digits, less to the carpal-metacarpal regions, and not at all to more proximal regions (Fig. 4K). By contrast, under the same conditions, Meis2a±Pbx1-electroporated cells contributed mainly to the carpal-metacarpal and less to the digit region (Fig. 4K). The ability of Meis overexpression to modify the contribution of regenerating limb cells is thus not confined to sorting between stylopod/zeugopod versus more distal regions, but is also detected within distal limb regions.

The results show that PD cell sorting or migration is the major cause of the proximal-preferential distribution of Meis-overexpressing cells. The ability of Meis to modify limb cell PD affinity during regeneration is active throughout the PD axis of the regenerating limb. Our results suggest a role for

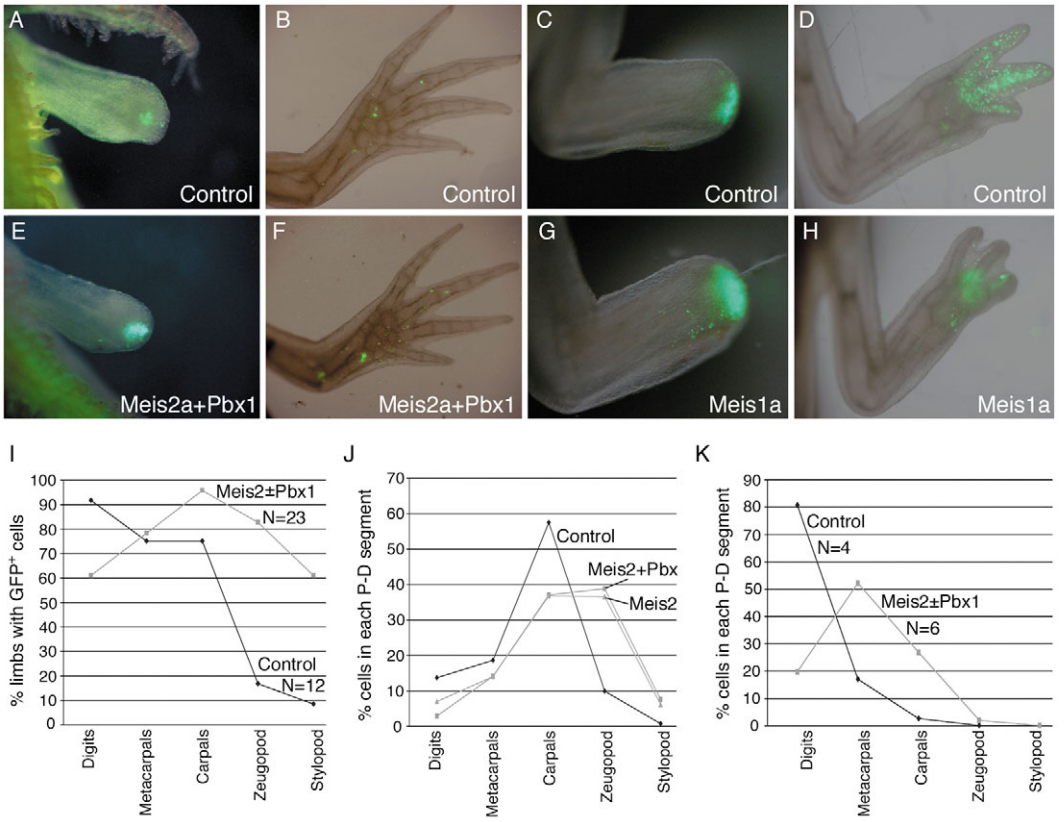

Fig. 4. Meis overexpression induces distal-to-proximal relocation of blastema cells. (A,E) Mid-humerus medium bud blastemas 1 day after focal electroporation of EGFP (A) or Meis2+Pbx1+EGFP (E). (B,F) The same limbs after complete regeneration. (C,G) Distal early bud blastemas one day after bulk electroporation with EGFP or EGFP+Meis1a. (D,H) The same limbs after complete regeneration. (I) Proportion of limbs showing GFP-positive cells in the different PD limb segments after focal electroporation of EGFP or Meis2±Pbx1+EGFP. (J) Percentage of GFP-positive cells in each PD segment of the limbs shown in I. (K) Percentage of GFP-positive cells within the different PD segments after focal electroporation of EGFP or Meis2±Pbx1+EGFP in the distal region of a late-bud proximal blastema.

Pbx1 in stabilizing Meis proteins and show that Pbx1 expression is not sufficient to promote proximal relocation.

Meis activity is required for RA-induced proximalization of distal blastemas

To study the consequences of Meis knockdown during RA-induced proximalization of the limb blastema, morpholino oligonucleotides (MO) that inhibit Meis1 and Meis2 protein expression in vivo (Fig. 5) were used in regeneration experiments. Fluorescently labeled MOs electroporated much more efficiently into blastema cells than did plasmid DNA, with up to 80% of cells showing a strong signal after electroporation (Fig. 6A,B). Using this approach, we determined the consequences of Meis1 and Meis2 knockdown during limb regeneration. When Meis1 MO (n=20), Meis2 MO (n=20), or both MOs (n=38), were electroporated into early-bud proximal blastemas, no alterations in the regeneration pattern were observed (not shown).

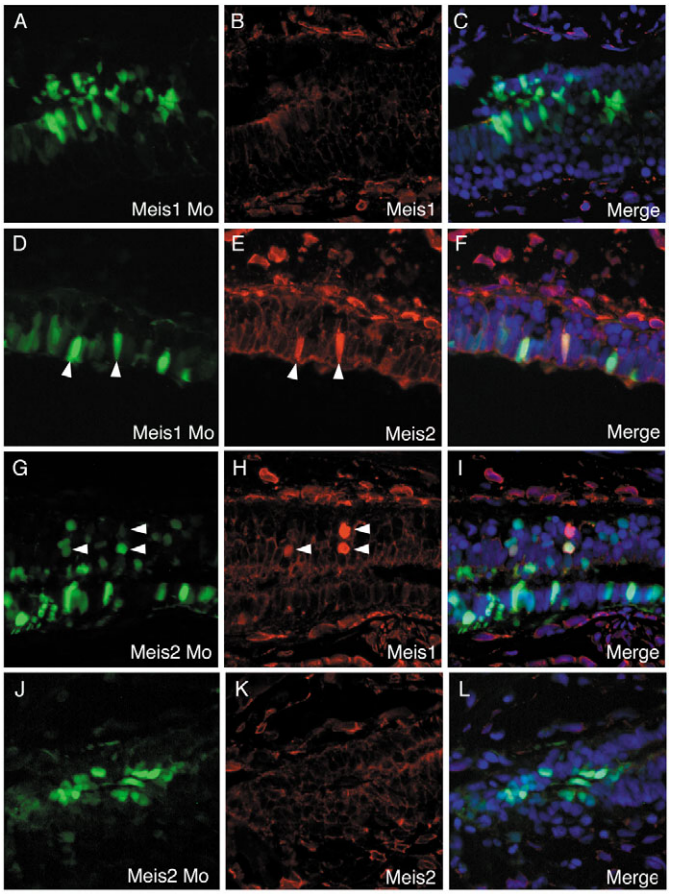

Fig. 5. Anti-Meis1 and anti-Meis2 morpholinos specifically block axolotl Meis1 and Meis2 translation. *Meis1* or *Meis2* constructs were co-electroporated together with anti-Meis1 or anti-Meis2 fluorescein-tagged MOs into the neural tube. Sagittal neural tube sections show MO-positive cells in green (A,D,G,J), Meis in red (B,E,H,K), and both signals merged with nuclear staining in blue (C,F,I,L). Arrowheads indicate Meis-positive cells. When Meis1 MO was co-electroporated with the Meis1 expression plasmid, no Meis1 protein expression was detected in MO-loaded cells (A-C). Instead, when Meis1 MO was co-electroporated with the Meis2 expression plasmid, MO and Meis2 protein signals were found in the same cells (D-F). Reciprocally, when Meis2 MO was co-electroporated with the Meis1 expression plasmid, MO and Meis2 protein signals were found in the same cells (G-I). Instead, when Meis2 MOs were co-electroporated with Meis2 expression plasmid, no Meis2 protein expression was detected in MO-loaded cells (J-L). These results indicate the effectiveness and specificity of the Meis1 and Meis2 MOs.

We next studied the consequences of Meis knockdown in the context of RA-induced PD tandem duplications. To generate PD duplications, axolotl larvae forelimbs were amputated at mid-carpal level and RA (100 μg/g body weight) was administered intraperitoneally 4 days after amputation. These conditions gave rise to tandem PD duplications, ranging from partial zeugopod to the complete PD axis, including shoulder elements. To score duplication intensity, we used a duplication index (DI) modified from that of Maden (Maden, 1983): partial zeugopod, 1; total zeugopod, 2; partial stylopod, 3; total stylopod, 4; shoulder element present, 5.

Bilateral amputations were performed, and left and right DI scored after regeneration following RA injection. Differences in degree between left and right duplication were determined by calculating the asymmetry index (AI; left DI minus right DI). Positive AI values indicate stronger duplications in the left limb; negative AI values indicate the opposite. When both left and right limbs were electroporated with control MO, deviations from symmetry were minor (never more than one AI unit in a single animal), and were balanced between left and right sides, so that the average AI was 0 (Fig. 6D, Fig. 7A,B). By contrast, when blastemas on one side were electroporated with control MO and those on the opposite with different combinations of Meis MO, less intense duplications were observed in the Meis MO-electroporated limbs in over half of the cases (Fig. 6C,E). This reduction in the DI affected animals showing any degree of duplication on the control side (Fig. 6E and not shown). The average AI was –0.8 for Meis1 and –1.0 for Meis2, when Meis MOs were electroporated on the left side (Fig. 7C,D). When Meis1 and Meis2 MOs were co-electroporated, the average AI variation was –0.8 when introduced on the left and +1 when introduced on the right. In all cases, DI reductions induced by *Meis1* and/or *Meis2* knockdown in single animals ranged from 1 to 3 duplication units, and affected 26 out of 46 treated animals (Fig. 7).

These results show that Meis knockdown does not result in an altered pattern of normal regeneration but indicate that Meis genes act downstream of RA to induce the proximalization of the regenerating limb.

Discussion

During limb regeneration, positional information must be re-specified to achieve a correctly patterned regenerated structure. A plausible scenario is that adult tissue re-uses the molecular machinery employed during development to pattern the re-growing body part (Bryant et al., 2002; Gardiner et al., 2002). Indeed, grafting experiments suggest that early limb bud and blastema cells share similar differentiation programs (Muneoka and Bryant, 1982), and developmentally active genes, such as the signaling molecules Fgf8 and Shh, as well as the Hox, Tbx and Dlx transcription factors, are re-expressed during regeneration (Beauchemin and Savard, 1992; Brown and Brockes, 1991; Gardiner et al., 1995; Han et al., 2001; Simon et al., 1997; Simon and Tabin, 1993; Torok et al., 1999).

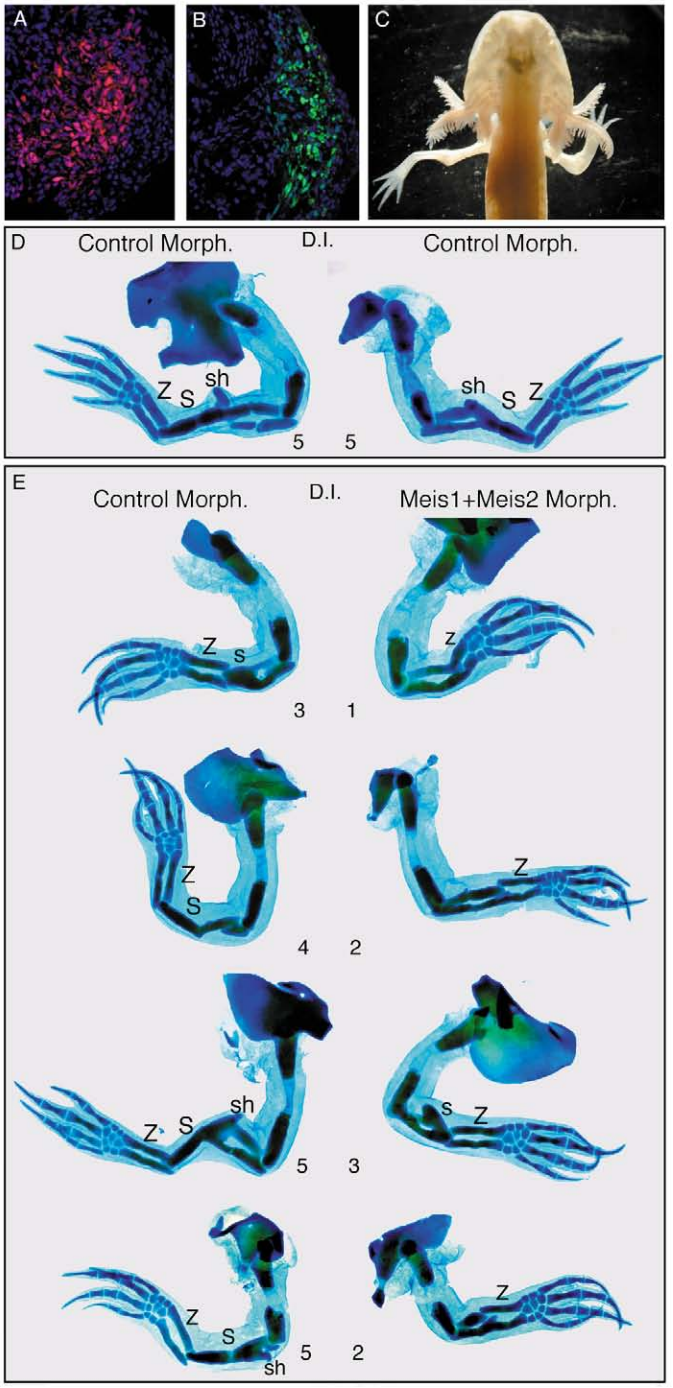

Fig. 6. Blockade of Meis gene function inhibits RA-induced blastema proximalization. (A,B) Longitudinal sections through distal limb blastemas, 30 hours post-electroporation with rhodamine-coupled control MO (A) or fluorescein-anti-Meis1+Meis2 MOs (B). (C) Dorsal view of an axolotl amputated bilaterally at mid-carpal level, RA-treated, and electroporated with Meis1+Meis2 MOs (right) and control MO (left). (D) Skeletal preparations of forelimbs from a single animal regenerated after RA treatment and bilateral electroporation with control MO. (E) Skeletal preparations of forelimbs regenerated after RA treatment and electroporated with control MO (left) and Meis1+Meis2 MOs (right). Each pair is from a single animal. Numbers beneath forelimbs indicate duplication indexes. S, complete extra stylopod; s, partial extra stylopod; sh, extra shoulder girdle; Z, complete extra zeugopod; z, partial extra zeugopod.

Here, we show that two closely related homeodomain proteins, Meis1 and Meis2, act as proximalizing factors during regeneration. When overexpressed, Meis proteins induce relocation to proximal regions of otherwise distal cells, a phenomenon also promoted by RA pathway activation (Crawford and Stocum, 1988; Pecorino et al., 1996). Meis knockdown inhibits RA proximalizing activity, showing that these genes represent key targets in the RA proximalizing pathway. By contrast, Meis knockdown induced no alterations in normal regeneration after a proximal amputation. One possible explanation for this result is that the RA-Meis pathway does not play any role during normal regeneration and thus its ability to reprogram distal blastemas would only correspond to the re-activation of an embryonic proximalizing pathway. However, our data do not exclude a role for Meis genes in establishing the proximal identity within the normal blastema. Indeed, when proximal stumps are confronted with distal blastemas in recombination experiments, instead of an interstitial deletion, normal regeneration takes place by intercalation of the missing identities from the stump (Iten and Bryant, 1975; Pescitelli and Stocum, 1981; Stocum, 1975). By contrast, when distal stumps are confronted with proximal blastemas, PD tandem duplications are obtained. In the light of these recombination experiments, in the case of an experimental distalization of the blastema, normal limb regeneration is still expected to occur, whereas in the case of an attenuation of an RA-induced proximalization, a change in the regeneration pattern is predicted. Further research is therefore necessary to establish the involvement of the RA-Meis pathway in normal regeneration.

During vertebrate limb development, *Meis1* and *Meis2* act downstream of RA in a proximalizing pathway (Mercader et al., 2000). Our results here show that the same pathway used during limb development is re-used in regeneration to specify proximal identity. In contrast to its effect on urodele limb regeneration, RA does not induce obvious PD duplications in the developing chick limb. A possible explanation is that during normal limb development, reprogrammed cells have the chance to migrate and integrate into proximal compartments, whereas during regeneration, they are ‘trapped’ in a distal region and are thus forced to generate an ectopic proximal compartment.

During amniote limb development, the limit of *Meis* gene expression in the patterned chicken limb corresponds to the boundary between the stylopod and the zeugopod. Localized inhibition of RA signaling in the chick disrupts skeletal elements proximal to the elbow/knee, but does not affect regions distal to this point. Conversely, localized RA excess disrupts elements distal to the elbow/knee but spares elements proximal to this point (Mercader et al., 2000). These results suggested a major subdivision of the limb bud into an RA-Meis domain that generates regions proximal to the stylopod/zeugopod boundary, and an RA-Meis-negative area that generates regions beyond this boundary. We found here that Meis gene expression and regulation through RA is conserved between amniote and amphibian limb development. Nonetheless, in the chick, RA exposure or Meis overexpression does not impose a stylopod character, but proximalizes cells at any distal position in a

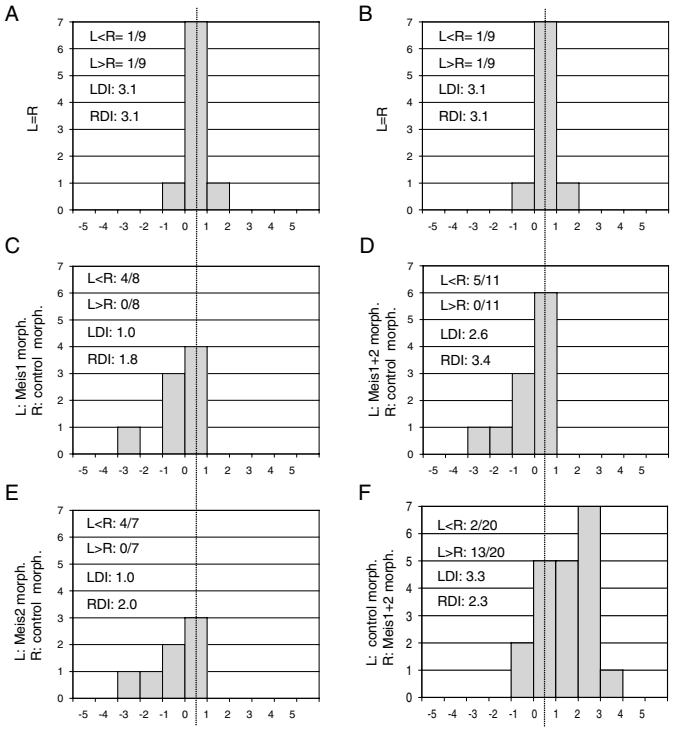

Fig. 7. Effect of Meis gene function blockade on RA-induced limb duplication. Graphs indicate the number of forelimb pairs (*y* axis) for the different asymmetry index values (*x* axis). (A) Bilateral control MO electroporation (repeated in B for reference), (C) Meis1 MO (left) and control MO (right), (E) Meis2 MO (left) and control MO (right), (D) Meis1+Meis2 MO (left) and control MO (right), (F) control MO (left) and Meis1+Meis2 MO (right). L, left; R, right; LDI, left duplication index; RDI, right duplication index.

graded manner (Mercader et al., 1999). Similar results are obtained after RA exposure during limb regeneration; duplications induced by decreasing amounts of RA result in increasing distalization of the proximal-most identity of the regenerate (Thoms and Stocum, 1984). The alterations in PD identity promoted by changes in Meis activity seem to follow similar rules; Meis overexpression proximalizes cell affinity at any position of the regenerating PD axis, and Meis knockdown distalizes the proximal-most identity of the regenerate, irrespective of the initial specification status of the blastema. These observations suggest that positional information is encoded uniformly, and is recognized continuously along the PD axis during both limb development and regeneration. In addition, the components of the positional code appear to remain sensitive to the RA-Meis pathway at any PD position.

Meis regulation is mainly transcriptional in amniotes, whereas in the axolotl it appears to be at least partially by translational and/or by subcellular protein localization. Mouse Meis proteins and their *Drosophila* ortholog Hth are translated and imported into the nucleus constitutively, whereas mouse Pbx1 and its *Drosophila* ortholog Exd require Meis/Hth expression to be imported into the nucleus and become functional (Abu-Shaar et al., 1999; Berthelsen et al., 1999; Capdevila et al., 1999; Mercader et al., 1999; Rieckhof et al., 1997). Data from *Xenopus*, zebrafish and spiders provide examples of the opposite situation; Pbx/Exd proteins are expressed constitutively in the nucleus whereas Meis/Hth proteins remain in the cytoplasm by default, and become nuclear only after co-expression with Pbx/Exd (Maeda et al., 2002; Prpic et al., 2003; Vlachakis et al., 2001). These observations suggest that the mechanisms for the regulation of Meis and Pbx activity have remained labile during evolution. This flexibility would only be possible if, as suggested by most Meis/Pbx functional experiments, Meis and Pbx proteins always work together, with no functional independence for each partner. Any change in the ability of a partner to enter the nucleus on its own would have no functional consequence, and would thus be unrestricted during evolution. In our experiments, however, Pbx neither induced alterations in cell behavior nor substantially changed the phenotype induced by Meis protein overexpression. These results might indicate that Meis alone can reprogram limb cell PD identity, although it is most likely to interact with Pbx proteins constitutively expressed in limb blastemas.

Another interesting aspect of limb PD specification mechanisms is the regulation of cell affinity. PD axial level-specific affinity is a hallmark of PD identity, and is modulated by RA during development and regeneration. The fact that Meis rapidly induces cell relocation in the early blastema suggests that PD-specific affinity is already established at this stage. Cell lineage tracing and transplantation experiments have also suggested an early PD sub-division of the limb blastema (Echeverri and Tanaka, 2005). Alterations of Meis activity at later stages similarly induced cell relocation, but within a restricted subregion of the regenerate, suggesting progressive PD compartmentalization of the blastema, or progressive limitation in cell migratory ability.

The GPI-anchored Prod1 molecule is downstream of RA in the proximalizing pathway, at least as part of the PD affinity code (da Silva et al., 2002; Echeverri and Tanaka, 2005). Prod1 appears to form part of the positional memory system that enables blastema cells to ‘know’ which limb parts are missing. By contrast, we found no evidence of Meis genes as part of the positional memory system, suggesting that the Meis pathway belongs exclusively to the patterning network re-activated after amputation. In this case, after proximal amputation, the Meis pathway would be activated by the positional memory system, so that the initial Prod1 status may determine the level of Meis activation. The answers to these questions must await isolation of the axolotl Prod1 counterpart.

We thank R. Mueller for building the electrodes, K. Echeverri for advice on plasmid electroporation, E. Schnapp for advice on MO electroporation, E. Leonardo for technical help, the animal house personnel for support in setting up the axolotl colony, and C. Mark for editorial assistance. N.M. was supported by EU Marie Curie long-term and EMBO short-term fellowships. M.T. and N.M. are supported by grant SAF2003-04317 from the Spanish Ministerio de Educación y Ciencia. The Department of Immunology and Oncology was founded and is supported by the Spanish Council for Scientific Research (CSIC) and by Pfizer.

References

Abu-Shaar, M., Ryoo, H. D. and Mann, R. S. (1999). Control of the nuclear localization of extradenticle by competing nuclear import and export signals. *Genes Dev.* **13**, 935-945.

Beauchemin, M. and Savard, P. (1992). Two distal-less related homeobox-

containing genes expressed in regeneration blastemas of the newt. *Dev. Biol.* **154**, 55-65.

Berggren, K., McCaffery, P., Drager, U. and Forehand, C. J. (1999). Differential distribution of retinoic acid synthesis in the chicken embryo as determined by immunolocalization of the retinoic acid synthetic enzyme, RALDH-2. *Dev. Biol.* **210**, 288-304.

Berthelsen, J., Kilstrup-Nielsen, C., Blasi, F., Mavilio, F. and Zappavigna, V. (1999). The subcellular localization of PBX1 and EXD proteins depends on nuclear import and export signals and is modulated by association with PREP1 and HTH. *Genes Dev.* **13**, 946-953.

Brockes, J. P. (1997). Amphibian limb regeneration: rebuilding a complex structure. *Science* **276**, 81-87.

Brown, R. and Brockes, J. P. (1991). Identification and expression of a regeneration-specific homeobox gene in the newt limb blastema. *Development* **111**, 489-496.

Bryant, S. V., Endo, T. and Gardiner, D. M. (2002). Vertebrate limb regeneration and the origin of limb stem cells. *Int. J. Dev. Biol.* **46**, 887-896.

Bürglin, T. R. (1997). Analysis of TALE superclass homeobox genes (MEIS, PBC, KNOX, Iroquois, TGIF) reveals a novel domain conserved between plants and animals. *Nucleic Acids Res.* **25**, 4173-4180.

Capdevila, J., Tsukui, T., Rodriquez Esteban, C., Zappavigna, V. and Izpisua Belmonte, J. C. (1999). Control of vertebrate limb outgrowth by the proximal factor Meis2 and distal antagonism of BMPs by Gremlin. *Mol. Cell* **4**, 839-849.

Chang, C. P., Jacobs, Y., Nakamura, T., Jenkins, N. A., Copeland, N. G. and Cleary, M. L. (1997). Meis proteins are major in vivo DNA binding partners for wild-type but not chimeric Pbx proteins. *Mol. Cell. Biol.* **17**, 5679-5687.

Crawford, K. and Stocum, D. L. (1988). Retinoic acid coordinately proximalizes regenerate pattern and blastema differential affinity in axolotl limbs. *Development* **102**, 687-698.

da Silva, S. M., Gates, P. B. and Brockes, J. P. (2002). The newt ortholog of CD59 is implicated in proximodistal identity during amphibian limb regeneration. *Dev. Cell* **3**, 547-555.

Duboule, D. (2002). Making progress with limb models. *Nature* **418**, 492-493.

Echeverri, K. and Tanaka, E. M. (2003). Electroporation as a tool to study in vivo spinal cord regeneration. *Dev. Dyn.* **226**, 418-425.

Echeverri, K. and Tanaka, E. (2005). Proximodistal patterning during limb regeneration. *Dev. Biol.* **279**, 391-401.

Gardiner, D. M., Blumberg, B., Komine, Y. and Bryant, S. V. (1995). Regulation of HoxA expression in developing and regenerating axolotl limbs. *Development* **121**, 1731-1741.

Gardiner, D. M., Endo, T. and Bryant, S. V. (2002). The molecular basis of amphibian limb regeneration: integrating the old with the new. *Semin. Cell Dev. Biol.* **13**, 345-352.

Habermann, B., Bebin, A. G., Herklotz, S., Volkmer, M., Eckelt, K., Pehlke, K., Epperlein, H. H., Schackert, H. K., Wiebe, G. and Tanaka, E. M. (2004). An Ambystoma mexicanum EST sequencing project: analysis of 17,352 expressed sequence tags from embryonic and regenerating blastema cDNA libraries. *Genome Biol.* **5**, R67.

Han, M. J., An, J. Y. and Kim, W. S. (2001). Expression patterns of Fgf-8 during development and limb regeneration of the axolotl. *Dev. Dyn.* **220**, 40-48.

Ide, H., Wada, N. and Uchiyama, K. (1994). Sorting out of cells from different parts and stages of the chick limb bud. *Dev. Biol.* **162**, 71-76.

Iten, L. E. and Bryant, S. V. (1975). The interaction between the blastema and stump in the establishment of the anterior-posterior and proximal-distal organization of the limb regenerate. *Dev. Biol.* **44**, 119-147.

Knoepfler, P. S., Calvo, K. R., Chen, H., Antonarakis, S. E. and Kamps, M. P. (1997). Meis1 and pKnox1 bind DNA cooperatively with Pbx1 utilizing an interaction surface disrupted in oncoprotein E2a-Pbx1. *Proc. Natl. Acad. Sci. USA* **94**, 14553-14558.

Livak, K. J. and Schmittgen, T. D. (2001). Analysis of relative gene expression data using real-time quantitative PCR and the 2(–Delta Delta C(T)) Method. *Methods* **25**, 402-408.

MacLean, G., Abu-Abed, S., Dolle, P., Tahayato, A., Chambon, P. and Petkovich, M. (2001). Cloning of a novel retinoic-acid metabolizing cytochrome P450, Cyp26B1, and comparative expression analysis with Cyp26A1 during early murine development. *Mech. Dev.* **107**, 195-201.

Maden, M. (1982). Vitamin A and pattern formation in the regenerating limb. *Nature* **295**, 672-675.

Maden, M. (1983). The effect of vitamin A on the regenerating axolotl limb. *J. Embryol. Exp. Morphol.* **77**, 273-295.

Maeda, R., Ishimura, A., Mood, K., Park, E. K., Buchberg, A. M. and Daar, I. O. (2002). Xpbx1b and Xmeis1b play a collaborative role in hindbrain and neural crest gene expression in Xenopus embryos. *Proc. Natl. Acad. Sci. USA* **99**, 5448-5453.

Mercader, N., Leonardo, E., Azpiazu, N., Serrano, A., Morata, G., Martinez, C. and Torres, M. (1999). Conserved regulation of proximodistal limb axis development by Meis1/Hth. *Nature* **402**, 425-429.

Mercader, N., Leonardo, E., Piedra, M. E., Martínez-A, C., Ros, M. A. and Torres, M. (2000). Opposing RA and FGF signals control proximodistal vertebrate limb development through regulation of Meis genes. *Development* **127**, 3961-3970.

Mic, F. A., Sirbu, I. O. and Duester, G. (2004). Retinoic acid synthesis controlled by Raldh2 is required early for limb bud initiation and then later as a proximodistal signal during apical ectodermal ridge formation. *J. Biol. Chem.* **279**, 26698-26706.

Muneoka, K. and Bryant, S. V. (1982). Evidence that patterning mechanisms in developing and regenerating limbs are the same. *Nature* **298**, 369-371.

Myat, A., Henrique, D., Ish-Horowicz, D. and Lewis, J. (1996). A chick homologue of Serrate and its relationship with Notch and Delta homologues during central neurogenesis. *Dev. Biol.* **174**, 233-247.

Nardi, J. B. and Stocum, D. L. (1983). Surface properties of regenerating limb cells – evidence for gradation along the proximodistal axis. *Differentiation* **25**, 27-31.

Niazi, I. A. and Saxena, S. (1978). Abnormal hind limb regeneration in tadpoles of the toad, Bufo andersoni, exposed to excess vitamin A. *Folia Biol (Krakow)* **26**, 3-8.

Niederreither, K., McCaffery, P., Drager, U. C., Chambon, P. and Dolle, P. (1997). Restricted expression and retinoic acid-induced downregulation of the retinaldehyde dehydrogenase type 2 (RALDH-2) gene during mouse development. *Mech. Dev.* **62**, 67-78.

Niederreither, K., Vermot, J., Schuhbaur, B., Chambon, P. and Dolle, P. (2002). Embryonic retinoic acid synthesis is required for forelimb growth and anteroposterior patterning in the mouse. *Development* **129**, 3563-3574.

Nye, H. L., Cameron, J. A., Chernoff, E. A. and Stocum, D. L. (2003). Regeneration of the urodele limb: a review. *Dev. Dyn.* **226**, 280-294.

Oulad-Abdelghani, M., Chazaud, C., Bouillet, P., Sapin, V., Chambon, P. and Dollé, P. (1997). Meis2, a novel mouse Pbx-related homeobox gene induced by retinoic acid during differentiation of P19 embryonal carcinoma cells. *Dev. Dyn.* **210**, 173-183.

Pecorino, L. T., Entwistle, A. and Brockes, J. P. (1996). Activation of a single retinoic acid receptor isoform mediates proximodistal respecification. *Curr. Biol.* **6**, 563-569.

Pescitelli, M. J., Jr and Stocum, D. L. (1981). Nonsegmental organization of positional information in regenerating Ambystoma limbs. *Dev. Biol.* **82**, 69-85.

Prpic, N. M., Janssen, R., Wigand, B., Klingler, M. and Damen, W. G. (2003). Gene expression in spider appendages reveals reversal of exd/hth spatial specificity, altered leg gap gene dynamics, and suggests divergent distal morphogen signaling. *Dev. Biol.* **264**, 119-140.

Reynolds, K., Mezey, E. and Zimmer, A. (1991). Activity of the beta-retinoic acid receptor promoter in transgenic mice. *Mech. Dev.* **36**, 15-29.

Rieckhof, G. E., Casares, F., Ryoo, H. D., Abu-Shaar, M. and Mann, R. S. (1997). Nuclear translocation of extradenticle requires homothorax, which encodes an extradenticle-related homeodomain protein. *Cell* **91**, 171-183.

Rossant, J., Zirngibl, R., Cado, D., Shago, M. and Giguere, V. (1991). Expression of a retinoic acid response element-hsplacZ transgene defines specific domains of transcriptional activity during mouse embryogenesis. *Genes Dev.* **5**, 1333-1344.

Schnapp, E. and Tanaka, E. M. (2005). Quantitative evaluation of morpholino-mediated protein knockdown of GFP, MSX1, and PAX7 during tail regeneration in Ambystoma mexicanum. *Dev. Dyn.* **232**, 162-170.

Simon, H. G. and Tabin, C. J. (1993). Analysis of Hox-4.5 and Hox-3.6 expression during newt limb regeneration: differential regulation of paralogous Hox genes suggest different roles for members of different Hox clusters. *Development* **117**, 1397-1407.

Simon, H. G., Kittappa, R., Khan, P. A., Tsilfidis, C., Liversage, R. A. and Oppenheimer, S. (1997). A novel family of T-box genes in urodele amphibian limb development and regeneration: candidate genes involved in vertebrate forelimb/hindlimb patterning. *Development* **124**, 1355-1366.

Spallanzani, L. (1768). *Prodromo di un'opera da imprimersi sopra le riproduzioni animali.* Módena, Italy: nella Stamperia di Giovanni Montanari.

Stocum, D. L. (1975). Regulation after proximal or distal transposition of limb regeneration blastemas and determination of the proximal boundary of the regenerate. *Dev. Biol.* **45**, 112-136.

Stocum, D. L. (1984). The urodele limb regeneration blastema. Determination and organization of the morphogenetic field. *Differentiation* **27**, 13-28.
Swindell, E. C., Thaller, C., Sockanathan, S., Petkovich, M., Jessell, T. M. and Eichele, G. (1999). Complementary domains of retinoic acid production and degradation in the developing embryo. *Dev. Biol.* **216**, 282-296.
Tamura, K., Yokouchi, Y., Kuroiwa, A. and Ide, H. (1997). Retinoic acid changes the proximodistal developmental competence and affinity of distal cells in the developing chick limb bud. *Dev. Biol.* **188**, 224-234.
Thoms, S. D. and Stocum, D. L. (1984). Retinoic acid-induced pattern duplication in regenerating urodele limbs. *Dev. Biol.* **103**, 319-328.
Tickle, C. (2003). Patterning systems – from one end of the limb to the other. *Dev. Cell* **4**, 449-458.
Torok, M. A., Gardiner, D. M., Izpisua-Belmonte, J. C. and Bryant, S. V. (1999). Sonic hedgehog (shh) expression in developing and regenerating axolotl limbs. *J. Exp. Zool.* **284**, 197-206.
Vlachakis, N., Choe, S. K. and Sagerstrom, C. G. (2001). Meis3 synergizes with Pbx4 and Hoxb1b in promoting hindbrain fates in the zebrafish. *Development* **128**, 1299-1312.
Wagner, K., Mincheva, A., Korn, B., Lichter, P. and Popperl, H. (2001). Pbx4, a new Pbx family member on mouse chromosome 8 is expressed during spermatogenesis. *Mech. Dev.* **103**, 127-131.
Wilkinson, D. G. and Nieto, M. A. (1993). Detection of messenger RNA by in situ hybridization to tissue sections and whole mount. *Methods Enzymol.* **225**, 361-373.
Yashiro, K., Zhao, X., Uehara, M., Yamashita, K., Nishijima, M., Nishino, J., Saijoh, Y., Sakai, Y. and Hamada, H. (2004). Regulation of retinoic acid distribution is required for proximodistal patterning and outgrowth of the developing mouse limb. *Dev. Cell* **6**, 411-422.